# Anharmonic Motion in the Crystal Structure of 2-Mercaptopyridone

Martin Lutz*, Tom J. Smak, and Arnaud T. Sanderse

## Supplementary Materials

**Table S1.** Temperature-dependent unit cell determinations. At each temperature, a 360° φ-scan was performed with a rotation increment of 0.3°. The detector distance was kept fixed at 40 mm during the complete experiment. The unit cells were obtained from full intensity integrations with Eval15 [1] resulting in 3250–3512 reflections per temperature ($\theta_{max}$ = 30.43–30.78°). The cell parameters correspond to the $P2_1/c$ space group setting which is consistent with the literature [2].[1] Literature data are provided for comparison.

| T [K] | a [Å] | b [Å] | c [Å] | β [°] | V [Å$^3$] |
|---|---|---|---|---|---|
| 100 | 6.0245(3) | 6.2566(2) | 14.1095(7) | 101.803(3) | 520.58(4) |
| 120 | 6.0311(3) | 6.2626(2) | 14.1307(6) | 101.911(2) | 522.23(4) |
| 140 | 6.0379(3) | 6.2688(3) | 14.1515(5) | 102.030(2) | 523.88(4) |
| 160 | 6.0450(2) | 6.2754(2) | 14.1743(7) | 102.145(3) | 525.67(4) |
| 180 | 6.0523(3) | 6.2815(3) | 14.1990(10) | 102.254(3) | 527.51(5) |
| 200 | 6.0595(6) | 6.2862(5) | 14.223(2) | 102.360(5) | 529.21(10) |
| 220 | 6.0678(5) | 6.2926(4) | 14.254(2) | 102.503(5) | 531.32(10) |
| 240 | 6.0768(5) | 6.2991(4) | 14.282(2) | 102.644(4) | 533.45(9) |
| 260 | 6.0847(5) | 6.3038(7) | 14.3128(16) | 102.797(6) | 535.36(9) |
| **Literature data:** | | | | | |
| 298 (PYRIDS[3]) | 6.10 (±0.3%) | 6.31 (±0.3%) | 14.35 (±0.3%) | 103° 01’ (±5’) | |
| 298 (PYRIDS02[2]) | 6.113(5) | 6.325(5) | 14.400(9) | 103.1(1) | |
| 116 (PYRIDS03[4]) | 6.044(1) | 6.273(1) | 14.146(2) | 101.93 | 524.77 |
| 298 (PYRIDS11[2]) | 6.107(2) | 6.325(2) | 14.382(4) | 103.0(5) | |

1 At 200, 220, 240 and 260 K the $P2_1/n$ setting would give a β angle closer to 90°.

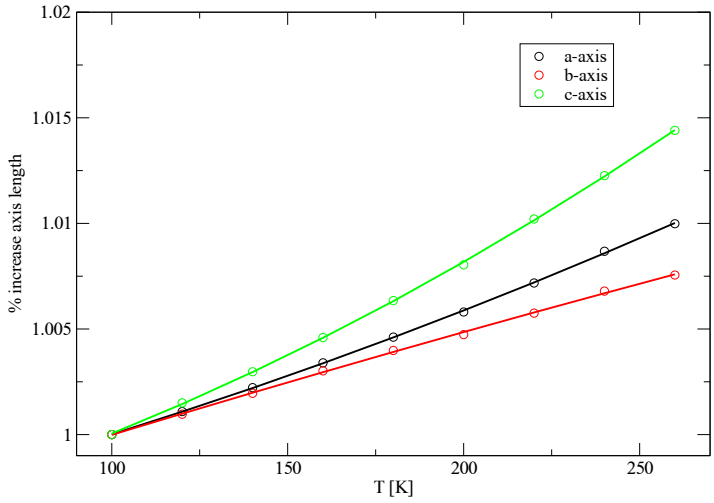


**Figure S1.** Temperature dependent development of unit cell parameters. The drawn lines were obtained from quadratic fits.

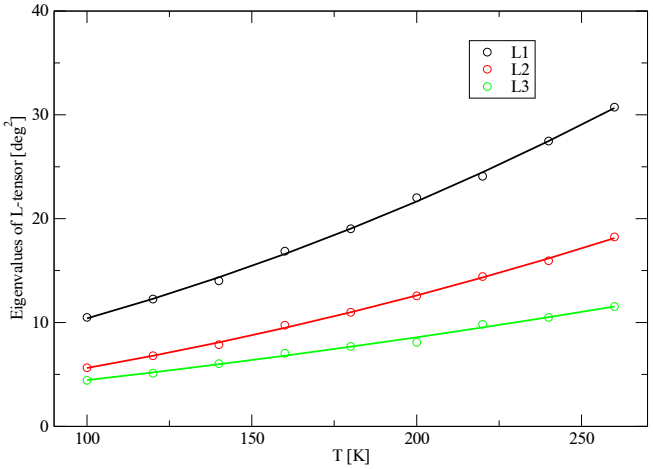


**Figure S2.** Temperature dependence of the L-tensor from a rigid-body TLS analysis. The analysis was performed with the routine CALC TMA in the PLATON software [5]. Drawn are the eigenvalues L1, L2 and L3 of the L-tensor. The lines were obtained from quadratic fits.

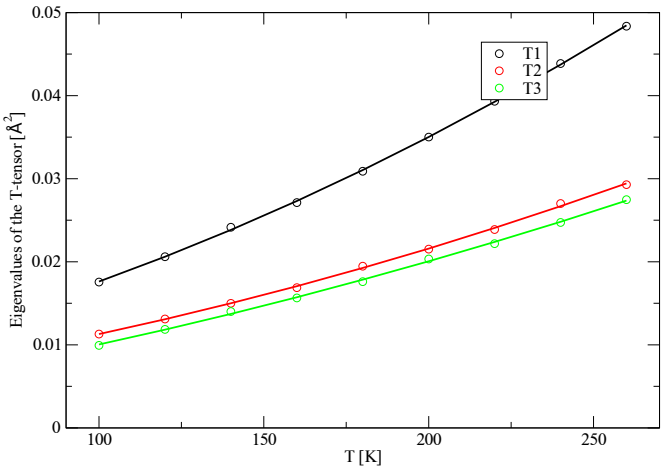


**Figure S3.** Temperature dependence of the T-tensor from a rigid-body TLS analysis. The analysis was performed with the routine CALC TMA in the PLATON software [5]. Drawn are the eigenvalues T1, T2 and T3 of the T-tensor. The lines were obtained from quadratic fits.

**Table S2.** Temperature dependence of the N−H···S hydrogen bond. Symmetry code *i*: −x, 1−y, −z.

| T [K] | N1−H1 [Å] | H1···S1$^{i}$ [Å] | N1····S1$^{i}$ [Å] | N1−H1···S1$^{i}$ [°] |
|---|---|---|---|---|
| 100 | 0.865(17) | 2.425(17) | 3.2728(9) | 166.6(14) |
| 120 | 0.864(17) | 2.427(16) | 3.2742(9) | 166.8(14) |
| 140 | 0.879(16) | 2.414(16) | 3.2743(9) | 166.2(13) |
| 160 | 0.873(16) | 2.420(16) | 3.2755(9) | 166.5(13) |
| 180 | 0.877(16) | 2.419(16) | 3.2761(9) | 165.5(14) |
| 200 | 0.862(16) | 2.438(16) | 3.2778(10) | 164.8(13) |
| 220 | 0.873(16) | 2.426(16) | 3.2787(10) | 165.5(13) |
| 240 | 0.868(16) | 2.436(16) | 3.2800(11) | 164.4(13) |
| 260 | 0.854(16) | 2.454(15) | 3.2818(11) | 163.4(13) |

**Table S3.** Temperature dependence of the intermolecular π···π stacking interaction. Cg: center of gravity of six-membered ring. Symmetry code *i*: −x, −y, −z. Cg_perp: perpendicular distance of Cg to the ring.

| T [K] | Cg···Cg$^{i}$ [Å] | Cg_perp [Å] | Slippage [Å] |
|---|---|---|---|
| 100 | 3.6708(6) | 3.3927(4) | 1.402 |
| 120 | 3.6770(6) | 3.4005(4) | 1.399 |
| 140 | 3.6827(6) | 3.4078(4) | 1.396 |
| 160 | 3.6886(6) | 3.4142(4) | 1.396 |
| 180 | 3.6953(7) | 3.4222(4) | 1.394 |
| 200 | 3.7014(8) | 3.4285(5) | 1.395 |
| 220 | 3.7103(9) | 3.4384(5) | 1.394 |
| 240 | 3.7172(9) | 3.4469(5) | 1.391 |
| 260 | 3.7258(9) | 3.4562(5) | 1.392 |

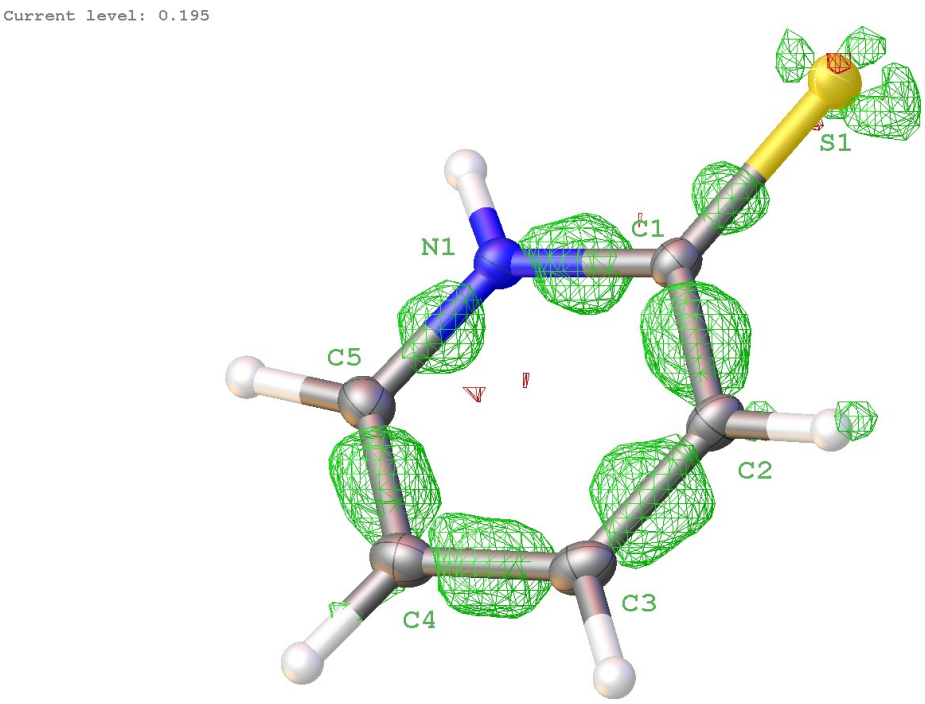


**Figure S4.** Difference electron density in **(I)**. Contour level 0.195 e/Å$^3$. Positive contours are drawn in green, negative in red. Calculated structure factors are taken from the spherical atom model refined with SHELXL [6]. Maximum resolution θ = 62°. Plot prepared with Olex2 [7].

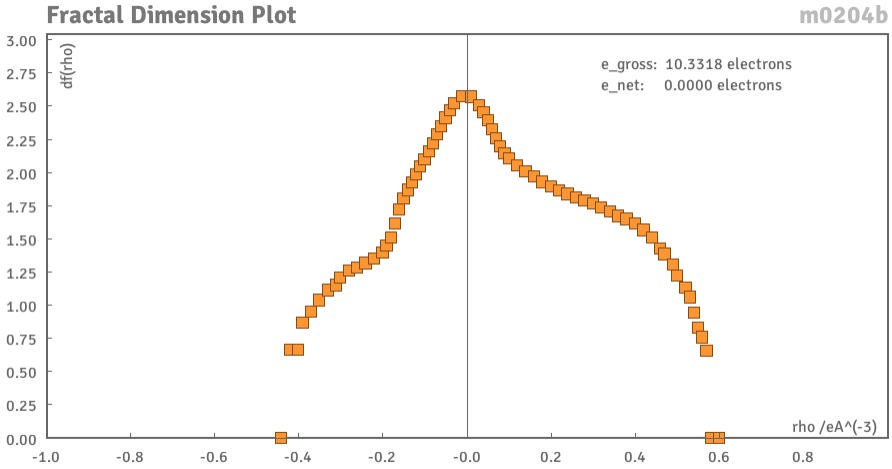


**Figure S5.** Fractal dimension plot [8] of the residual electron density from the spherical atom model. The same data as in Figure S4 were used. Plot prepared with Olex2 [7].

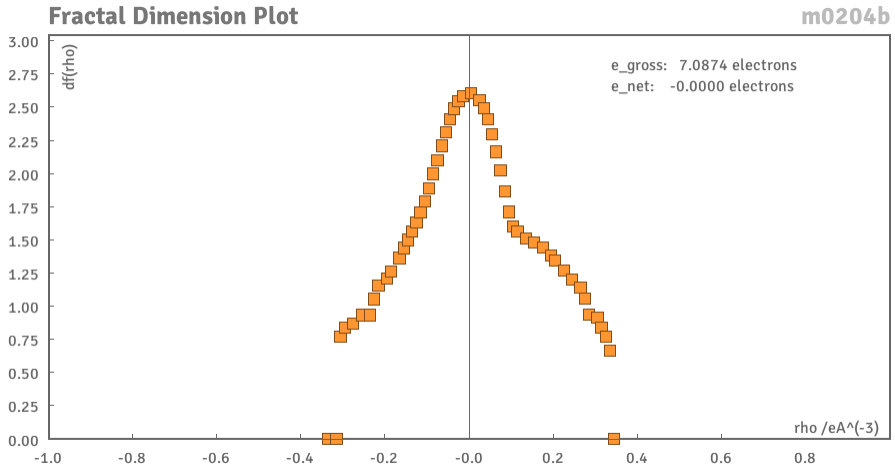


**Figure S6.** Fractal dimension plot [8] of the residual electron density from the non-spherical atom model (NoSpherA2). Plot prepared with Olex2 [7].

**Table S4.** Kitajgorodskij packing index (K.P.I.) [9] calculated with the PLATON software [5]. The analysis is based on the van-der-Waals radii of the atoms.

| | T [K] | C–H [Å] | K.P.I. |
|---|---|---|---|
| Present study: **I** (SHELXL) | 100 | 0.909(9)–1.008(8) | 71.5% |
| NOLZEV19 [10] (SHELXL) | 100 | 0.95 | 69.2% |

**Table S5.** Void calculation with CrystalExplorer (Version 21.5) [11]. Hydrogen atoms are normalized to standardized neutron distances. The calculation is based on the electron density from quantum chemical calculations. An isosurface of 0.002 e/au$^3$ was used.

| | V (unit cell) [Å$^3$] | V (void) [Å$^3$] | Void (percentage) |
|---|---|---|---|
| Present study: **I** | 521.243(9) | 27.74 | 5.3% |
| NOLZEV19 [10] | 1980.7(7) | 227.26 | 11.5% |

**Table S6.** Comparison of NoSpherA2 refinements with isotropic and anisotropic displacement parameters for the hydrogen atoms. $P = (F_o^2 + 2F_c^2)/3$.

| | NoSpherA2 ($H_{iso}$) | NoSpherA2 ($H_{aniso}$) |
|---|---|---|
| weighting scheme | $w = 1/[\sigma^2(F_o^2) + (0.0157P)^2 + 0.0052P]$ | $w = 1/[\sigma^2(F_o^2) + (0.0130P)^2 + 0.0049P]$ |
| no. of refl. | 8374 | 8374 |
| no. of param. | 84 | 109 |
| R1 [I>2σ(I)] | 0.0125 | 0.0116 |
| wR2 [I>2σ(I)] | 0.0308 | 0.0277 |
| R1 [all refl.] | 0.0155 | 0.0146 |
| wR2 [all ref.] | 0.0325 | 0.0292 |
| GooF | 1.0085 | 1.0097 |
| $\Sigma (\Delta^2/\sigma^2)$ | 44037.65 | 36141.70 |
| $\Delta\rho_{min/max}$ [e/Å$^3$] | –0.26/0.28 | –0.27/0.28 |

**Table S7.** Analysis of variance [12, 13]. The F-values are obtained from the internet [14].
$\mathscr{R} = \sqrt{([b/(n-m)] \times F_{b,n-m,\alpha} + 1)}$.

| | No. parameters (b) | deg. of freedom (n-m) | $\Sigma (\Delta^2/\sigma^2)$ |
|---|---|---|---|
| NoSpherA2 ($H_{iso}$) | 84 | 8374 – 84 = 8290 | 44037.65 |
| NoSpherA2 ($H_{aniso}$) | 109 | 8374 – 109 = 8265 | 36141.70 |
| Difference | 25 | 25 | 7895.95 |
| | | | |
| R-factor ratio | $\sqrt{(44037.65/36141.70)} = 1.1038$ | | |
| | | | |
| Significance α = 0.001 | F = 2.1085; $\mathscr{R}$ = 1.0032 | | |
| Significance α = 0.0005 | F = 2.2021; $\mathscr{R}$ = 1.0033 | | |

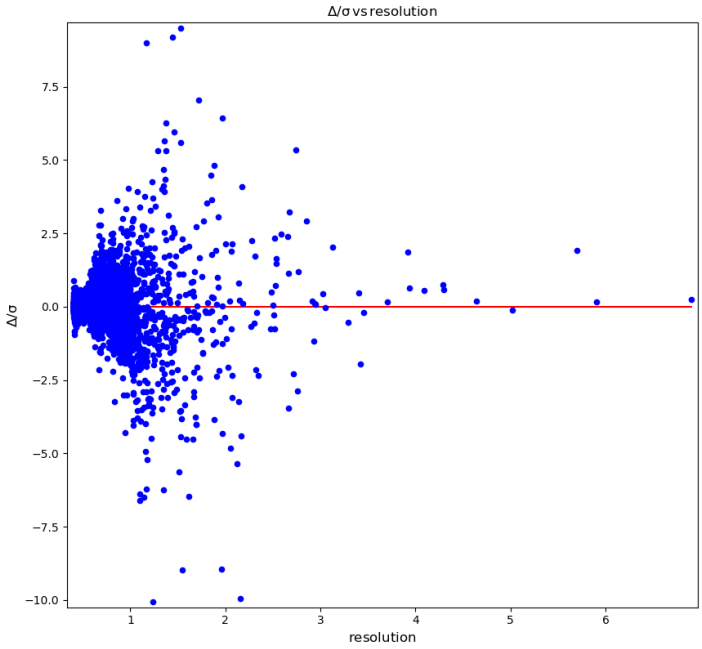


**Figure S7.** Comparison of calculated structure factors from NoSpherA2 refinements with isotropic and with anisotropic hydrogen atoms. $\Delta = F_{calc}^2$ (iso-H) – $F_{calc}^2$ (aniso-H). σ-values are taken from the merged reflection files. Resolution = sin θ / λ.

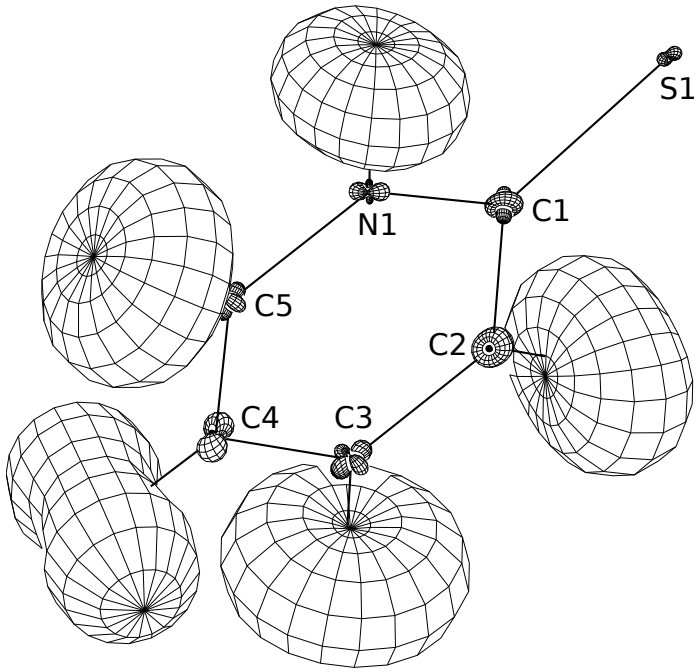


**Figure S8.** Peanut plot [15] of **I** (NoSpherA2 refinement). Shown is the difference between the refined anisotropic displacement parameters and a rigid-body TLS model (THMA11). The scale of the rmsd surfaces is 6.15.

**Table S8.** Analysis of variance [12, 13] for the multipole refinements. The F-values are obtained from the internet [14]. $\mathscr{R} = \sqrt{([b/(n-m)] \times F_{b,n-m,\alpha} + 1)}$.
Model A. Non-hydrogen atoms with multipoles up to hexadecapole level and anisotropic displacement parameters. Hydrogen atoms fixed on parameters from NoSpherA2.
Model B. Anharmonic motion for sulfur added (up to 3rd order).
Model C. Anharmonic motion for all non-hydrogen atoms added (up to 3rd order).
Model D. Anisotropic displacement parameters and multipoles up to quadrupole added for hydrogen atoms.

| | No. parameters (b) | deg. of freedom (n-m) | $\Sigma (\Delta^2/\sigma^2)$ |
|---|---|---|---|
| Model A | 252 | 8115 – 252 = 7863 | 36621.21 |
| Model B | 262 | 8115 – 262 = 7853 | 28652.95 |
| Difference | 10 | 10 | 7968.26 |
| | | | |
| R-factor ratio | $\sqrt{(36621.21/28652.95)} = 1.1305$ | | |
| | | | |
| Significance $\alpha = 0.001$ | $F = 2.9628$; $\mathscr{R} = 1.0019$ | | |
| Significance $\alpha = 0.0005$ | $F = 3.1467$; $\mathscr{R} = 1.0020$ | | |

| | No. parameters (b) | deg. of freedom (n-m) | $\Sigma (\Delta^2/\sigma^2)$ |
|---|---|---|---|
| Model B | 262 | 8115 – 262 = 7853 | 28652.95 |
| Model C | 322 | 8115 – 322 = 7793 | 25071.64 |
| Difference | 60 | 60 | 3581.31 |
| | | | |
| R-factor ratio | $\sqrt{(28652.95/25071.64)} = 1.0690$ | | |
| | | | |
| Significance $\alpha = 0.001$ | $F = 1.6646$; $\mathscr{R} = 1.0064$ | | |
| Significance $\alpha = 0.0005$ | $F = 1.7165$; $\mathscr{R} = 1.0066$ | | |

| | No. parameters (b) | deg. of freedom (n-m) | $\Sigma (\Delta^2/\sigma^2)$ |
|---|---|---|---|
| Model C | 322 | 8115 – 322 = 7793 | 25071.64 |
| Model D | 377 | 8115 – 377 = 7738 | 20870.48 |
| Difference | 55 | 55 | 4201.16 |
| | | | |
| R-factor ratio | $\sqrt{(25071.64/20870.48)} = 1.0960$ | | |
| | | | |
| Significance $\alpha = 0.001$ | $F = 1.6984$; $\mathscr{R} = 1.0060$ | | |
| Significance $\alpha = 0.0005$ | $F = 1.7533$; $\mathscr{R} = 1.0062$ | | |

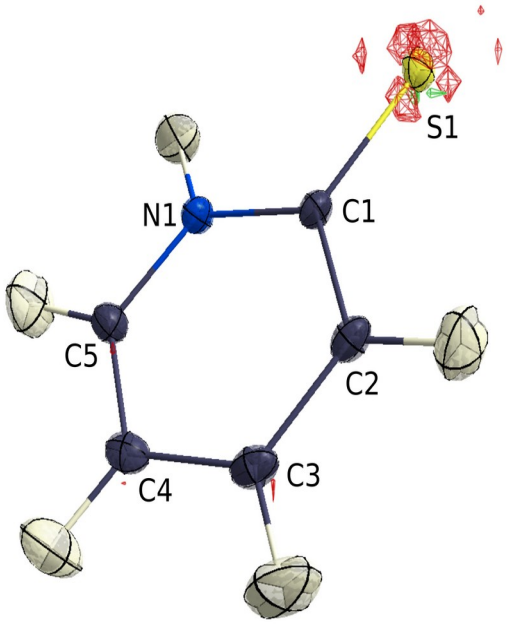


**Figure S9.** Residual density after multipole refinement. Contour level 0.13 e/Å$^3$. Positive values in green, negative values in red. Non-hydrogen atoms were refined with anisotropic displacement parameters and their multipoles up to the hexadecapole level. The plot was prepared with the MoleCoolQt software [16].

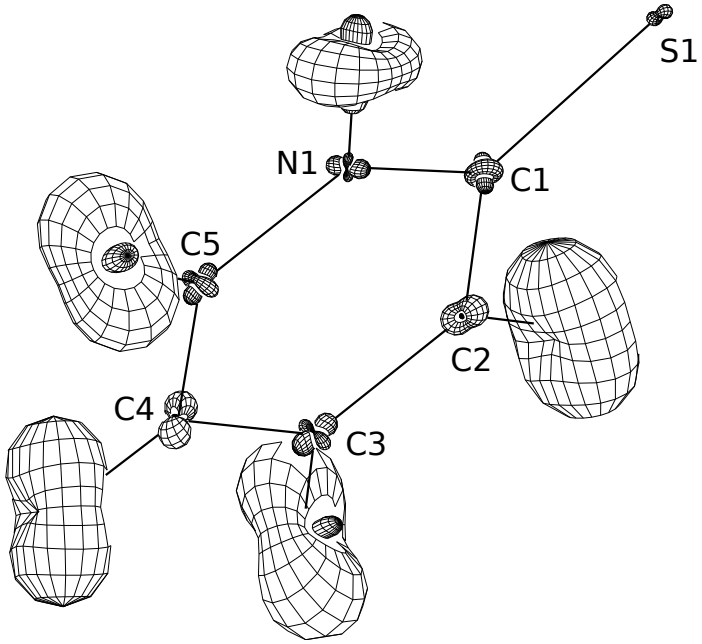


**Figure S10.** Peanut plot [15] of **I** (multipole refinement). Anisotropic hydrogen parameters were refined freely. Shown is the difference between the refined anisotropic displacement parameters and a rigid-body TLS model (THMA11). The scale of the rmsd surfaces is 6.15.

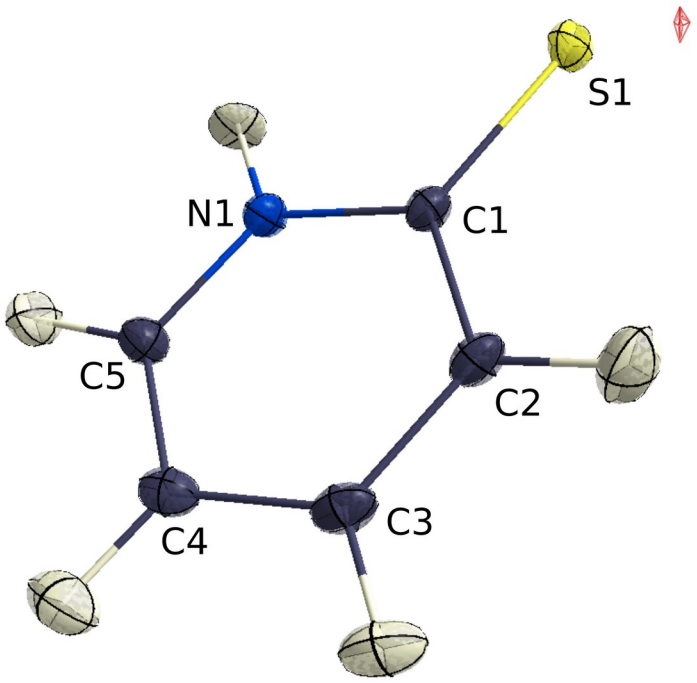


**Figure S11.** Residual density after the final multipole refinement. Contour level 0.13 e/Å$^3$. Non-hydrogen atoms were refined with anharmonic displacement parameters (3$^{rd}$ level) and their multipoles up to the hexadecapole level. Hydrogen atoms were refined with anisotropic displacement parameters. The plot was prepared with the MoleCoolQt software [16].

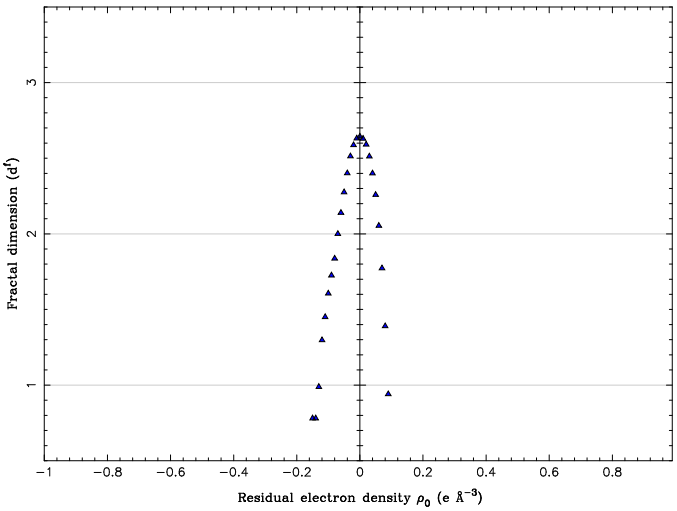


**Figure S12.** Fractal dimension plot [8] after the final multipole refinement, e_gross = 5.9750. Non-hydrogen atoms were refined with anharmonic displacement parameters (3$^{rd}$ level) and their multipoles up to the hexadecapole level. Hydrogen atoms were refined with anisotropic displacement parameters. The plot was prepared with WinXD [17].

**Table S9.** Temperature dependence of the intermolecular C–H···S contact. Symmetry code *i*: x–1, y, z.

| T [K] | C5–H5 [Å] | H5···S1$^{i}$ [Å] | C5····S1$^{i}$ [Å] | C5–H5···S1$^{i}$ [°] |
|---|---|---|---|---|
| 100 | 0.95 | 2.97 | 3.5704(12) | 122 |
| 120 | 0.95 | 2.98 | 3.5752(12) | 122 |
| 140 | 0.95 | 2.98 | 3.5815(12) | 122 |
| 160 | 0.95 | 2.99 | 3.5877(12) | 122 |
| 180 | 0.95 | 3.00 | 3.5931(12) | 122 |
| 200 | 0.95 | 3.00 | 3.5992(13) | 122 |
| 220 | 0.94 | 3.01 | 3.6057(14) | 122 |
| 240 | 0.94 | 3.02 | 3.6150(14) | 122 |
| 260 | 0.93 | 3.03 | 3.6211(14) | 123 |

# References


[1] Schreurs, A.M.M.; Xian, X.; Kroon-Batenburg, L.M.J. *EVAL15:* A diffraction data integration method based on ab initio predicted profiles. *J. Appl. Crystallogr.* **2010,** *43,* 70–82.

[2] Ohms, U.; Guth, H.; Kutoglu, A.; Scheringer, C. 2-Thiopyridone: X-ray and neutron diffraction study. *Acta Crystallogr. Sect. B* **1982,** *38*, 831–834.

[3] Penfold, B.R. The crystal structure of α-thiopyridone. *Acta Crystallogr.* **1953,** *6*, 707–713.

[4] Reynolds, J.G.; Sendlinger, S.C.; Murray, A.M.; Huffman, J.C.; Christou, G. Synthesis and Characterization of Vanadium(II,III,IV) Complexes of Pyridine-2-thiolate. *Inorg. Chem.* **1995,** *34*, 5745–5752.

[5] Spek, A.L. Structure validation in chemical crystallography. *Acta Crystallogr. Sect. D* **2009,** *65*, 148–155.

[6] Sheldrick, G.M. Crystal structure refinement with *SHELXL*. *Acta Crystallogr. Sect. C* **2015,** *71*, 3–8.

[7] Dolomanov, O.V.; Bourhis, L.J.; Gildea, R.J.; Howard, J.A.K.; Puschmann, H. *OLEX2:* A complete structure solution, refinement and analysis program. *J. Appl. Crystallogr.* **2009,** *42*, 339–341.

[8] Meindl, K.; Henn, J. Foundations of residual-density analysis. *Acta Crystallogr. Sect. A* **2008,** *64*, 404–418.

[9] Kitajgorodskij, A.I. *Molecular Crystals and Molecules*. Academic Press, New-York, 1973.

[10] Schillmöller, T.; Ruth, P.N.; Herbst-Irmer, R. and Stalke, D. Analysis of Solid-State Luminescence Emission Amplification at Substituted Anthracenes by Host–Guest Complex Formation. *Chemistry – A European Journal* **2020,** *26*, 17390-17398.

[11] Spackman, P.R.; Turner, M.J.; McKinnon, J.J.; Wolff, S.K.; Grimwood, D.J.; Jayatilaka, D.; Spackman, M.A. *CrystalExplorer:* A program for Hirshfeld surface analysis, visualization and quantitative analysis of molecular crystals. *J. Appl. Crystallogr.* **2021,** *54,* 1006–1011.

[12] Hamilton, W.C. Significance tests on the crystallographic *R* Factor. *Acta Crystallogr.* **1965,** *18,* 502–510.

[13] Destro, R.; Roversi, P.; Barzaghi, M.; Lo Presti, L. Anharmonic Thermal Motion Modelling in the Experimental XRD Charge Density Determination of 1-Methyluracil at T = 23 K. *Molecules* **2021,** *26,* 3075.

[14] Soper, D. S. *Critical F-Value Calculator*, https://www.danielsoper.com/statcalc (accessed on 26/02/2022), 2022.

[15] Hummel, W.; Hauser, J. and Bürgi, H.-B. *PEANUT:* Computer graphics program to represent atomic displacement parameters. *Journal of Molecular Graphics* **1990,** *8,* 214-220.

[16] Hübschle, C.B.; Dittrich, B. *MoleCoolQt*—A molecule viewer for charge-density research. *J. Appl. Crystallogr.* **2011,** *44*, 238–240.

[17] Farrugia, L.J. *WinXD*, University of Glasgow, 2016.